Report

Osmotic Regulation of Rab-Mediated Organelle Docking

Christopher L. Brett[1] and Alexey J. Merz[1],*
[1]Department of Biochemistry
University of Washington
Seattle, Washington 98195-7350

Summary

Osmotic gradients across organelle and plasma membranes modulate the rates of membrane fission and fusion; sufficiently large gradients can cause membrane rupture [1–6]. Hypotonic gradients applied to living yeast cells trigger prompt (within seconds) swelling and fusion of *Saccharomyces cerevisiae* vacuoles, whereas hypertonic gradients cause vacuoles to fragment on a slower time scale [7–11]. Here, we analyze the influence of osmotic strength on homotypic fusion of isolated yeast vacuoles. Consistent with previously reported in vivo results, we find that decreases in osmolyte concentration increase the rate and extent of vacuole fusion in vitro, whereas increases in osmolyte concentration prevent fusion. Unexpectedly, our results reveal that osmolytes regulate fusion by inhibiting early Rab-dependent docking or predocking events, not late events. Our experiments reveal an organelle-autonomous pathway that may control organelle surface-to-volume ratio, size, and copy number: Decreasing the osmolyte concentration in the cytoplasmic compartment accelerates Rab-mediated docking and fusion. By altering the relationship between the organelle surface and its enclosed volume, fusion in turn reduces the risk of membrane rupture.

Results

Organelle-Autonomous Regulation of Fusion by Osmolyte Concentration

The yeast vacuole is, like the mammalian lysosome, the terminal compartment of the endocytic pathway. Our cell-free fusion system (Figure S1, available online) places purified yeast vacuoles in a standard reaction buffer containing physiological salts, 200 mM sorbitol, and ATP. Decreasing the sorbitol concentration in the buffer increased the extent (Figure 1A) and rate (Figure 1B) of fusion. Conversely, increasing the sorbitol concentration decreased the extent and rate of fusion and lengthened the lag time prior to fusion (Figure 1B). Quantitative morphometry (Figure 1C) of fusion reactions corroborated the results from content-mixing assays. These in vitro results closely mirror observations of living cells [7–11]. The inhibitory effect of sorbitol is due to osmotic strength rather than sorbitol's specific physical or chemical properties. Replacement of sorbitol with other small polar osmolytes, including trehalose, glycerol, and sucrose (Figure S2A; unpublished data), yielded results comparable to sorbitol. Glycerol and trehalose are present at up to several percent (wt/vol) in living yeast cells [12], indicating that they are not intrinsic

*Correspondence: merza@u.washington.edu

inhibitors of membrane traffic. Dissolved solutes alter viscosity and, through excluded-volume and hydration effects, the chemical activity of water [13, 14]. A 15% solution of dextran-5 is more viscous than a 15% solution of sorbitol but has less than one-tenth as much osmotic strength; it slightly stimulated fusion (Figure S2A). Thus, viscosity per se does not prevent fusion. The results obtained with dextran-5 and bovine serum albumin (Figure S2A) further indicate that excluded-volume effects [13, 14] cannot explain inhibition by sorbitol. Excluded-volume and hydration effects also shift the ionic optima of many enzymatic reactions. Fusion is most efficient at ~125 mM KCl; this sharp ionic optimum did not shift appreciably as the sorbitol concentration was varied (Figure S2B). Thus, small polar solutes decrease the rate of fusion by increasing osmotic strength. This effect is organelle autonomous, requiring neither cytosol nor an intact plasma membrane.

Osmotic Control of an Early Docking or Predocking Subreaction

To map the osmotic effect to specific subreactions of fusion (Figure S1), we performed kinetic studies with stage-specific inhibitors (Figure 2A). A master fusion reaction was initiated. At intervals, reaction aliquots were transferred to tubes containing the specified treatments, incubated further, and assayed for fusion. This approach tracks loss of susceptibility to each treatment, i.e., the kinetics of completion of each subreaction. Treatments that modulate only early subreactions exhibit kinetics shifted left of the anti-Vam3 (docking) curve. Treatments that modulate later subreactions map between the anti-Vam3 and "ice" (content-mixing) curves. Unexpectedly, 1.4 M sorbitol inhibited fusion at early but not late time points (Figure 2A). After 20 min, fusion was less than 90% resistant to sorbitol addition, even though docking (anti-Vam3 curve) was less than 80% complete and content mixing (ice curve) was only ~30% complete. Lowering sorbitol to 100 mM yielded identical kinetics: Fusion was accelerated at early times but not late times.

Because the osmotic effect mapped to early docking, we hypothesized that osmolytes modulate the kinetics of early- or intermediate-stage subreactions. To test this hypothesis, we assayed subreaction kinetics at three sorbitol concentrations (Figure 2B). The earliest subreaction, Sec18- and Sec17-mediated priming [15, 16], was not substantially influenced by osmotic strength. Sec17 release from the membrane, a biochemical correlate of priming, was also unaltered (Figure 2B, inset). All subsequent stages of the reaction were accelerated by reduced sorbitol concentration (100 mM versus 200 mM sorbitol) and slowed as sorbitol was added: tethering and docking (rGdi1, an inhibitor of Rab GTPases); *trans*-SNARE complex formation (anti-Vam3); and content mixing (MARCKS effector-domain peptide [MED] [17]). Thus, osmolytes regulate early docking and change the kinetics of Rab-mediated subreactions. We next asked whether osmolytes regulate tethering, operationally defined by the formation of clusters of associated vacuoles [9, 18]. Consistent with the kinetic and staging data, increasing buffer osmolarity strongly decreased the efficiency of tethering (Figure 2C).
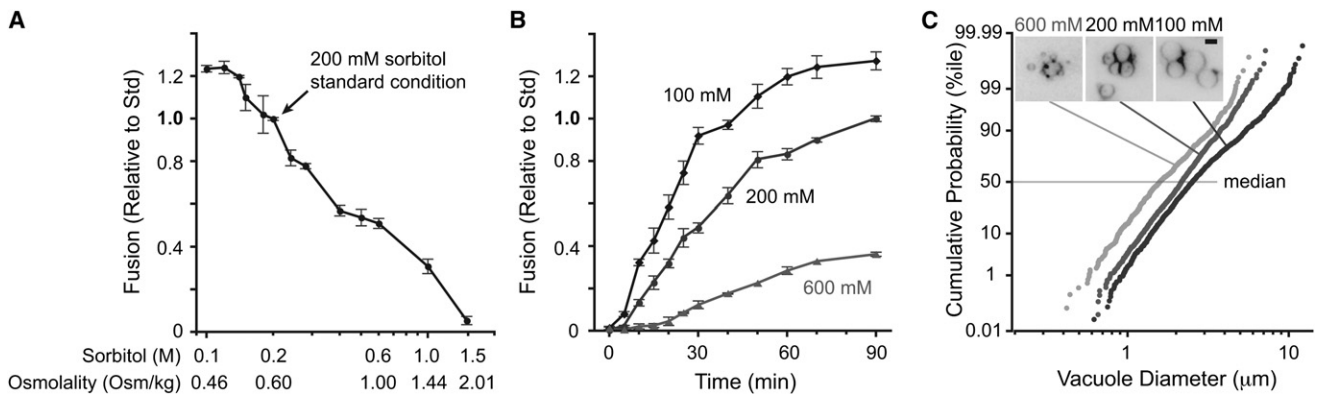
Figure 1. Osmotic Control of Homotypic Vacuole Fusion

(A) In vitro homotypic vacuole fusion at the indicated concentrations of sorbitol was measured after a 90 min incubation. On the horizontal axis, measured buffer osmolality is shown for reaction buffers containing the indicated concentrations of sorbitol. $n \geq 4$ for each point.

(B) Kinetics of fusion in hypotonic (100 mM), standard (200 mM), and hypertonic (600 mM sorbitol) conditions. $n \geq 4$ for each point; bars indicate SEM.

(C) Vacuole diameter increases with fusion. Fusion increases both membrane area and volume, and hence the size of the vacuoles in the population. To crosscheck the results obtained in content-mixing assays, we measured vacuole diameter at the end of 70 min fusion reactions containing the indicated concentrations of sorbitol. The morphometric data are plotted in rank order in cumulative probability histograms, with the median vacuole diameter (50th percentile) for each treatment indicated. We measured 500–1000 vacuoles from at least two experiments for each condition. The inset shows examples of morphology of FM4-64-stained vacuoles after 70 min incubation with ATP. The scale bar represents 2.5 μm.

Osmolytes Functionally Destabilize Ypt7:GTP and the HOPS Complex

To further evaluate the molecular basis of the link between osmotic strength and fusion, we measured dosage sensitivities for several fusion inhibitors at four sorbitol concentrations (Figure 3 and Figure S3). Osmolyte did not systematically change the IC_{50} (50% inhibitory concentration) for affinity-purified antibodies raised against the priming factor Sec17 (Figures S3A and S3C) or against the SNARE Vam3 (Figures 3A and 3C). Unaltered IC_{50} values were also obtained for MED peptide [17], a late-stage inhibitor of fusion that chelates acidic phospholipids (Figure S3B). In contrast, dose-response relationships for two Rab-specific inhibitors, the Rab-chelating chaperone rGdi1 and the GTPase activating protein (GAP) $rGyp1_{TBC}$, were closely linked to osmotic strength. IC_{50} values for rGdi1 and $rGyp1_{TBC}$ increased by nearly an order of magnitude as osmolyte was decreased (Figure 3C; compare Figure 3A to Figure 3B). Consistent with this result, in vivo overproduction of a second Ypt7 GAP, Gyp7, caused superinhibition of vacuole fusion by osmolyte, both in intact cells and in cell-free assays (unpublished data). Thus, osmolytes inhibit Rab-regulated subreactions of fusion.

The Ypt7 effector complex HOPS is anchored to the membrane by active Ypt7:GTP, so membrane association of HOPS provides a functional proxy for Ypt7 activation [19, 20]. Differential centrifugation experiments revealed that HOPS subunits were stabilized on membranes at low osmotic strength but dissociated into the supernatant as osmotic strength was increased (Figure 4A). Additional experiments with the Rab chaperone rGdi and experiments with the poorly hydrolyzable GTP analog GTPγS (which stabilizes activated Ypt7) further support this interpretation (unpublished data). Taken together, the data indicate that osmolytes functionally and biochemically destabilize Ypt7:GTP and its HOPS effector complex.

Rab Hyperactivation or Bypass Partially Reverses Osmotic Effects

We asked whether treatments that increase the quantity of active Rab GTPase or attenuate the Rab requirement could restore fusion at elevated osmotic strength. First, we exploited our previous finding that the recombinant SNARE rVam7 bypasses the priming requirement for ATP [21, 22]. rVam7 also reduces the Rab requirement and stabilizes HOPS on the vacuole membrane [21–24]. At elevated sorbitol concentrations, rVam7 restored fusion to approximately half the level observed under the standard condition (Figure 4B, top). At lower sorbitol concentrations (100 mM), rVam7 slightly suppressed fusion. This effect might result from SNARE-mediated lysis [24].

Second, we tested whether osmolyte-mediated inhibition is attenuated when there is more active Rab on the vacuole membrane. Gyp7 is the major Ypt7 GAP in vivo, and vacuoles purified from *gyp7Δ* cells have elevated levels of both Ypt7:GTP and HOPS (unpublished data). When fusion of vacuoles from *gyp7Δ* cells was measured at different concentrations of osmolyte, the effect of osmolyte was attenuated, as with rVam7 addition (Figure 4B, middle). Moreover, addition of rVam7 to vacuoles isolated from *gyp7Δ* cells had an additive effect, resulting in fusion at elevated osmotic strength that approached the standard condition (data not shown).

Third, we exploited the finding that removal of the vacuolar casein kinase I Yck3 dramatically reduces the requirement for Ypt7:GTP both in vitro [11] and in vivo (unpublished data). Vacuoles isolated from *yck3Δ* mutant cells (Figure 4B, bottom), like vacuoles from *gyp7Δ* mutants, fused more robustly than vacuoles from wild-type cells as the osmolyte concentration increased. Hence, the inhibitory effect of osmotic strength is attenuated by three independent manipulations that either stabilize the activated Rab or decrease the Rab requirement.

Discussion

Osmoregulation of docking and fusion is widespread, but the mechanisms of osmotic sensing and the molecular targets of this regulation are unknown. In *Paramecium*, membrane tension generated by osmotic pressure was hypothesized to trigger cycles of vacuole exocytosis for locomotion [2]. In mammalian cells, the rapid coalescence of intracellular
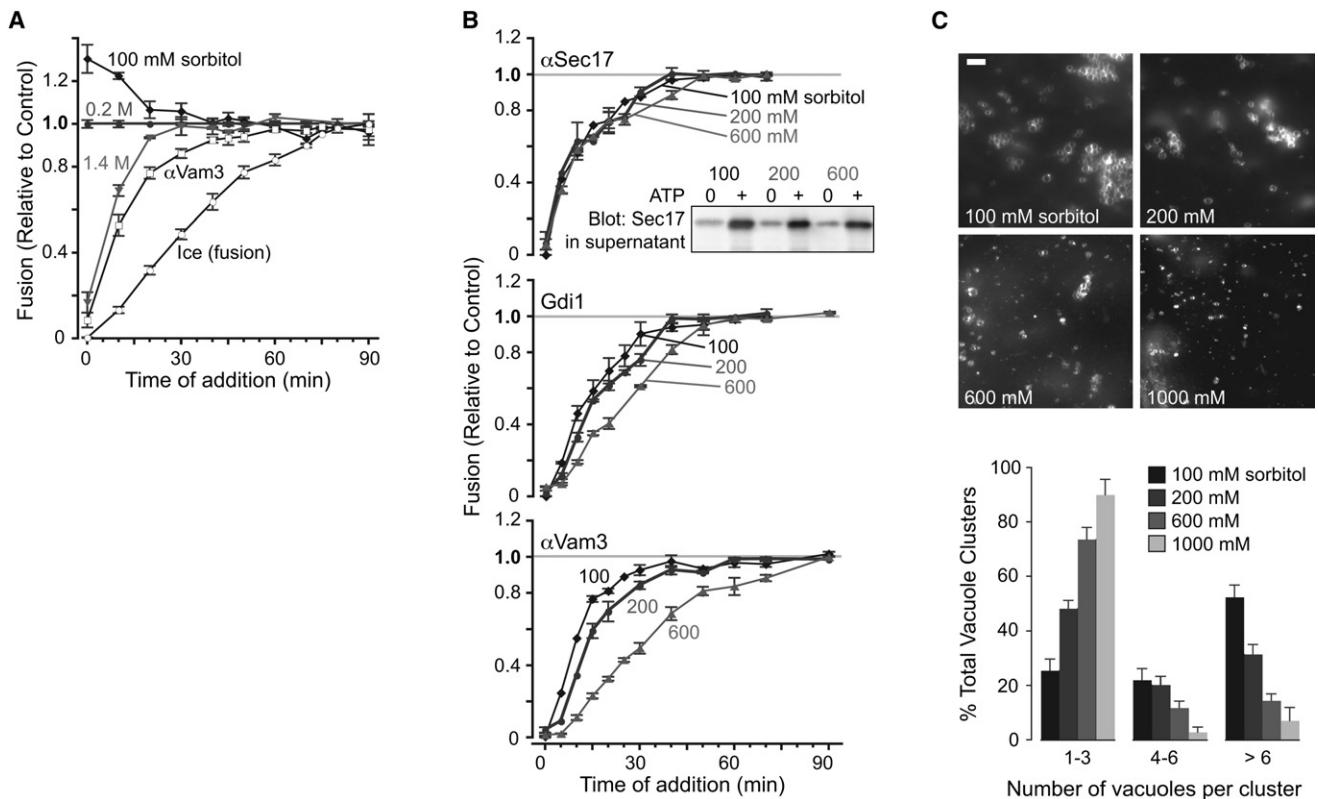
Figure 2. Osmotic Control of Early Docking Subreactions

(A) Kinetic mapping of osmotic effect. At the times indicated, aliquots of standard vacuole fusion reactions (200 mM sorbitol) were shifted to a final sorbitol concentration of 100, 200, or 1400 mM, as indicated, and incubated for a total of 90 min. Data are normalized to the values obtained with reactions diluted in isotonic (200 mM sorbitol) buffer. Kinetics are also shown for inhibitors of docking (Vam3 antibody, 35 nM) and fusion (ice) at standard 200 mM sorbitol. n ≥ 4 independent experiments.

(B) Osmotic control of docking kinetics. At the indicated times, subreaction inhibitors were added to reactions containing 100, 200, or 600 mM sorbitol throughout the incubation. Fusion inhibitors include the following (from early- to late-stage inhibition): 322 nM Sec17 antibody, 14 μM rGdi1, and 35 nM Vam3 antibody. The data are normalized to fusion values obtained in control samples, to which fusion buffer was added in place of inhibitor at the indicated times (gray lines). The inset shows vacuoles that were incubated with or without ATP for 10 min in the presence of 100, 200, or 600 mM sorbitol and then sedimented. The amount of Sec17 released from the membrane pellet was determined by western blot analysis with one-sixth of the supernatant from each fusion reaction. n ≥ 4 independent experiments.

(C) Osmotic inhibition of tethering. Images show FM4-64-stained vacuoles after 30 min of incubation with or without ATP in the presence of 100, 200, 600, or 1000 mM sorbitol. The scale bar represents 6 μm. Vacuole clusters were scored under each condition, and data are presented as a percentage of the total. A cluster refers to a single group of vacuoles. At least 200 clusters were counted for each condition. Error bars denote means ± SEM.

organelles, triggered by hypo-osmotic gradients, was reported almost a century ago [1]. There is a general correlation between low osmolarity in the cytoplasm or high osmolarity in an extracytoplasmic compartment and fusion [3–6]. For example, exocytosis is triggered by extracytoplasmic osmolytes, such as sucrose [5, 6], and inhibited by osmolyte in the cytoplasmic compartment [3]. In this study, we found that osmotic shifts influence fusion when applied during early docking but are without effect during later subreactions. Taken together, our experiments show that osmolytes can control an organelle's docking machinery in an organelle-autonomous manner, and they are fully consistent with earlier in vivo observations [7–11].

In principle, osmosensors could operate directly, e.g., by detecting changes in hydration, or indirectly, by sensing changes in membrane properties as osmotic gradients cause water and ionic species to flow across a membrane. Dai et al. recorded spontaneous lateral tension changes of ~40 μN/m during exocytosis and endocytosis in rat basophilic leukemia

cells [4]. Both organelle-organelle and exocytotic fusion events introduce slack into the product membrane, increasing the surface-to-volume ratio of the organelle or cell. This in turn increases the capacity for inward water movement without lysis. Thus, the ability of the docking machinery to respond to osmolytes may serve to prevent membrane tension from rising to perilous (lytic) levels during osmotic stress. Lytic tension for lysosomes and vacuoles may be lower than for other membranes because lysis might be accelerated by lipases and other hydrolases that reside within the organelle lumen. Hypo-osmotic stress can rupture lysosomes, to catastrophic effect [25], and experiments by Starai and coworkers [24] demonstrated that SNARE overabundance promotes membrane rupture, indicating that even normal membrane traffic functions are not without hazards. Coupling the activity of the docking machinery to cytoplasmic osmolyte concentration or to transmembrane osmotic gradients may be central to maintenance of organelle surface-to-volume relationships and membrane integrity.
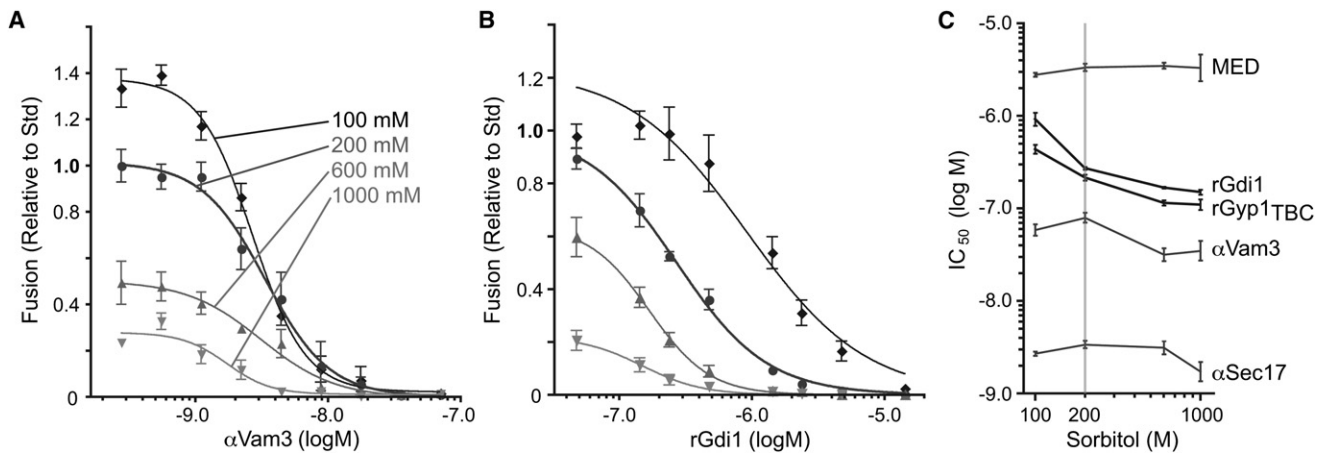
Figure 3. Osmolytes Enhance Sensitivity of Fusion to Rab Inhibitors

(A and B) Homotypic vacuole fusion was measured after vacuoles were incubated with ATP for 90 min in the presence of 100, 200, 600, or 1000 mM sorbitol and increasing concentrations of (A) Vam3 antibody or (B) rGdi1. Sigmoidal dose-response curves were fit to the data sets.

(C) IC_{50} values were extracted from the fits shown in (A) and (B) and from similar curves for other inhibitors (see Figures S3A–S3C). Bars span 95% confidence intervals; $n \geq 4$ for all experiments shown. Dose response for additional inhibitors and an alternative presentation of the IC_{50} values is presented in Figure S3D.

Experimental Procedures

Yeast Strains

For fusion assays, we used complimentary strain pairs of either BJ3505 (*MATα pep4::HIS3 prb1-1.6R his3–200 lys2–801 trp1101* (*gal3*) *ura3–52 gal2 can1*) and DKY6281 (*MATα leu2–3 leu 2–112 ura3–52 his3-200 trp1-901 lys2–801*) or BY4742 *pho8Δ* and BY4742 *pep4Δ* (*MAT α ura3Δ leu2Δ his3Δ lys2Δ pep4Δ::neo*; Invitrogen, Carlsbad, CA). BJ3505 *gyp7Δ::URA3* and DKY6281 *gyp7Δ::URA3* were gifts from Dr. Dieter Gallwitz (Max Planck Institute of Biophysical Chemistry, Göttingen, Germany). BY4742 *yck3Δ pho8Δ* (= AMY809) and BY4742 *yck3Δ pep4Δ* (= AMY807) were constructed by crossing and sporulating BY4741 *yck3Δ* (*MATa his3Δ leu2Δ met15Δ ura3Δ yck3Δ::neo*; Invitrogen) against BY4742 *pep4Δ::neo* or BY4742 *pho8Δ::neo*. Genotypes of the resulting haploid strains were confirmed by PCR and DNA sequencing.

Reagents

All biochemical reagents were purchased from Sigma-Aldrich (St. Louis, MI) or Invitrogen, except as indicated, and were of biotechnology grade or better. The endoglucanase fraction of Zymolyase 20T (Seikigaku Kogyo, Tokyo, Japan) was purified by cation-exchange chromatography before use in vacuole isolation. Purified proteins used include recombinant Vam7 (rVam7 [21]; unpublished data); recombinant Gdi1 (rGdi1) purified from bacterial cells with a CBP-intein fusion system provided by V. Starai and W. Wickner; recombinant catalytic domain of Rab-GAP Gyp1 (rGyp1$_{TBC}$) [19]; synthetic MARCKS Effector Domain peptide [17]; and recombinant protease inhibitor Pbi2. Rabbit polyclonal sera raised against Vps41, Vps33, Vps18, Vps11, Ypt7, Sec17, and Vam3 were gifts from W. Wickner (Dartmouth College, Hanover, NH), and were affinity purified and in some cases crossadsorbed against cell lysates from corresponding yeast deletion mutants to eliminate crossreactivity. The protein reagents used in fusion assays were prepared in 10 mM Pipes-KOH (pH 6.8) 200 mM sorbitol (PS) or were exchanged into this buffer by dialysis or size-exclusion chromatography.

Fusion

Vacuoles were purified as described [26]. Isolated vacuoles (6 μg) were incubated for 90 min at 27°C in standard reaction buffer: PS buffer
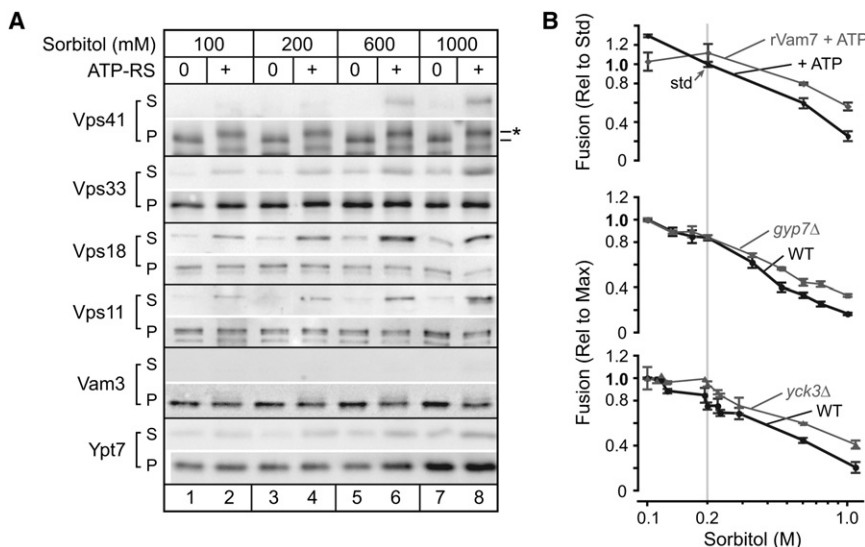

Figure 4. Interplay between Osmotic Strength and Docking Factors

(A) Osmolyte-triggered HOPS dissociation from the vacuole. Vacuoles were incubated with or without ATP for 70 min in the presence of 100, 200, 600, or 1000 mM sorbitol and then sedimented. Membrane association of 4 HOPS components (Vps41, Vps33, Vps18, and Vps11), a vacuole Q_a-SNARE (Vam3), and the vacuole Rab GTPase (Ypt7) was assessed by western blot with one-third of the total isolated supernatant (S) and one-tenth (0.6 μg vacuole protein) of the pellet (P). Phospho-Vps41 (*) was observed exclusively in the presence of ATP, as reported [11]. (B) Rab activation or partial Rab bypass attenuates inhibition by osmolyte. Top: Vacuoles were incubated for 90 min with ATP at increasing sorbitol concentrations in the presence and absence of recombinant Q_c-SNARE rVam7, which reduces the Ypt7 requirement in fusion [21, 22]. Middle and bottom: Vacuoles were purified from yeast strains containing or lacking Gyp7 (middle), which, when absent, stabilizes membrane association of Ypt7 and components of HOPS (unpublished data) or the vacuolar casein kinase I Yck3 (bottom), which, when absent, stabilizes HOPS on the membrane [11]. Fusion data were normalized to either the mean rate of fusion under standard conditions (ATP only, 200 mM sorbitol; top) or conditions where maximum fusion values were observed (100 mM sorbitol; middle, bottom). $n \geq 4$ for each point; error bars denote means ± 95% confidence intervals.

supplemented with salts (5 mM $MgCl_2$, 125 mM KCl), CoA (10 mM), and Pbi2 (with or without ATP-regenerating system [1 mM ATP, 0.1 mg/ml creatine kinase, 40 mM creatine phosphate]). Vacuoles were always added last to a premixed reaction cocktail, unless otherwise specified. Bypass fusion was initiated with recombinant Vam7 (100 nM, except as indicated). Osmotic gradients were imposed by reducing or adding sorbitol to the standard fusion reaction buffer (200 mM sorbitol). Like sorbitol, KCl concentrations were adjusted without compensatory equiosmolar changes in other buffer constituents. The solution's total osmolalities (Figure 1A and Table S1) were measured with a Vapro 5520 vapor-pressure osmometer (Wescor, Logan, UT). As indicated, reactions also contained rGdi1, $rGyp1_{TBC}$, Sec17 antibody, Vam3 antibody, $rGyp1_{TBC}$, MED, or GTPγS. Total volume of each fusion reaction was 30 μl. Fusion reactions were prepared with BY4742 $pho8\Delta$ (or DKY6128; alkaline phosphatase deficient) and $pep4\Delta$ (or BJ3505; protease deficient) vacuoles (3 μg each), with or without genomic deletion of $YCK3$ ($yck3\Delta$) or $GYP7$ ($gyp7\Delta$). Homotypic vacuole fusion was measured with a biochemical complementation assay ([26]; see [18] for quantitative characterization of the reporter system). Fusion (content mixing) was quantified by measuring the ALP-catalyzed evolution of p-nitrophenolate at 400 nm. Signals were then subtracted from a background control reaction either lacking ATP or incubated on ice; the signal-to-background ratio under our standard conditions routinely exceeds 25:1. Results are reported relative to signals obtained under standard fusion conditions (200 mM sorbitol with ATP), unless otherwise indicated. Under standard conditions, the mean extent of fusion was 3.5 (n = 98) fusion units as defined previously, corresponding to approximately two rounds of fusion [18, 26]. In addition, we verified that sorbitol does not alter the efficiency of ALP activation in assays with vacuole lysates (data not shown) [18]. Vacuole membrane release of Sec17, Ypt7, and HOPS components was assessed with fusion reactions containing only protease-deficient vacuoles (6 μg $pep4\Delta$ or BJ3505). After incubation at 27°C for 10 min, 40 min, or 70 min, fusion reactions were immediately sedimented by centrifugation at 20,000 × g for 5 min at 4°C. Pellet and supernatant fractions were fractionated by SDS-PAGE and analyzed by immunoblotting.

Microscopy

To examine vacuole morphology in vitro, we incubated $pep4\Delta$ vacuoles for times indicated (30 min or 70 min) at 27°C in fusion reaction buffer containing 3.0 μM FM4-64. After incubation, reactions were placed on ice. Then 2 μl of each reaction was mixed with 0.4% agarose, mounted on a chilled glass coverslip, and immediately imaged. Vacuole diameters and contact-zone lengths were measured from micrographs subjected to high-pass and sharpening filters with Image/J v. 1.36b software (Wayne Rasband, National Institutes of Health (NIH), Wachington, DC). Vacuole-clustering analysis was performed as described [9] with minor modifications: No cytosol was added to reactions, and KCl was not reduced to 40 mM. In brief, 5 μg of $pep4\Delta$ vacuoles were incubated at 27°C for 30 min in reaction buffer containing $MgCl_2$ (1.0 mM) and FM4-64 (3.0 μM) in the absence or presence of a lower than conventional concentration of ATP-regenerating system (0.6 mM ATP). Then 2 μl of the reaction was imaged as described above. Micrographs were acquired with an Olympus IX71 light-microscope system outfitted with an EMCCD (Andor iXon), ultrabright green- and blue-light-emitting diodes (>350 mW output) synchronized with the camera by custom electronics, a PlanApoN 1.45 NA 60× objective lens, and AndorIq v. 6.0.3.62 software (Andor Bioimaging, Nottingham, UK). Micrographs were processed with Image/J v. 1.36b (J. Rasband, NIH, http://rsb.info.nih.gov/ij/) and PhotoshopCS v. 8.0 (Adobe Systems) software.

Data Analysis

Where applicable, data sets were fit to sigmoidal dose-response functions with a nonlinear least-squares algorithm. log IC_{50} estimates were extracted from the sigmoidal fits with Prism v. 4.0c software (GraphPad, San Diego, CA). Statistical comparisons were performed with two-tailed Student's t tests (paired or unpaired, as appropriate); significance was assumed at the 5% level, after Dunn-Sidak compensation for repeated comparisons.

Supplemental Data

Supplemental Data include four figures and one table and can be found with this article online at http://www.current-biology.com/cgi/content/full/18/14/1072/DC1/.

References

1. Hogue, M.J. (1919). The effect of hypotonic and hypertonic solutions on fibroblasts of the embryonic chick heart in vitro. J. Exp. Med. *30*, 617–648.
2. Tominaga, T., Allen, R.D., and Naitoh, Y. (1998). Cyclic changes in the tension of the contractile vacuole complex membrane control its exocytotic cycle. J. Exp. Biol. *201*, 2647–2658.
3. Zimmerberg, J., Sardet, C., and Epel, D. (1985). Exocytosis of sea urchin egg cortical vesicles in vitro is retarded by hyperosmotic sucrose: Kinetics of fusion monitored by quantitative light-scattering microscopy. J. Cell Biol. *101*, 2398–2410.
4. Dai, J., Ting-Beall, H.P., and Sheetz, M.P. (1997). The secretion-coupled endocytosis correlates with membrane tension changes in RBL 2H3 cells. J. Gen. Physiol. *110*, 1–10.
5. Fatt, P., and Katz, B. (1952). Spontaneous subthreshold activity at motor nerve endings. J. Physiol. *117*, 109–128.
6. Bekkers, J.M., and Stevens, C.F. (1989). NMDA and non-NMDA receptors are co-localized at individual excitatory synapses in cultured rat hippocampus. Nature *341*, 230–233.
7. Bone, N., Millar, J.B., Toda, T., and Armstrong, J. (1998). Regulated vacuole fusion and fission in Schizosaccharomyces pombe: An osmotic response dependent on MAP kinases. Curr. Biol. *8*, 135–144.
8. Wang, Y.X., Kauffman, E.J., Duex, J.E., and Weisman, L.S. (2001). Fusion of docked membranes requires the armadillo repeat protein Vac8p. J. Biol. Chem. *276*, 35133–35140.
9. Wang, L., Seeley, E.S., Wickner, W., and Merz, A.J. (2002). Vacuole fusion at a ring of vertex docking sites leaves membrane fragments within the organelle. Cell *108*, 357–369.
10. Roberts, C.J., Raymond, C.K., Yamashiro, C.T., and Stevens, T.H. (1991). Methods for studying the yeast vacuole. Methods Enzymol. *194*, 644–661.
11. LaGrassa, T.J., and Ungermann, C. (2005). The vacuolar kinase Yck3 maintains organelle fragmentation by regulating the HOPS tethering complex. J. Cell Biol. *168*, 401–414.
12. Hounsa, C.G., Brandt, E.V., Thevelein, J., Hohmann, S., and Prior, B.A. (1998). Role of trehalose in survival of Saccharomyces cerevisiae under osmotic stress. Microbiology *144*, 671–680.
13. Ellis, R.J. (2001). Macromolecular crowding: Obvious but underappreciated. Trends Biochem. Sci. *26*, 597–604.
14. Parsegian, V.A., Rand, R.P., and Rau, D.C. (1995). Macromolecules and water: Probing with osmotic stress. Methods Enzymol. *259*, 43–94.
15. Mayer, A., Wickner, W., and Haas, A. (1996). Sec18p (NSF)-driven release of Sec17p (a-SNAP) can precede docking and fusion of yeast vacuoles. Cell *85*, 83–94.
16. Sollner, T., Bennett, M.K., Whiteheart, S.W., Scheller, R.H., and Rothman, J.E. (1993). A protein assembly-disassembly pathway in vitro that may correspond to sequential steps of synaptic vesicle docking, activation, and fusion. Cell *75*, 409–418.
17. Fratti, R.A., Jun, Y., Merz, A.J., Margolis, N., and Wickner, W. (2004). Interdependent assembly of specific regulatory lipids and membrane fusion proteins into the vertex ring domain of docked vacuoles. J. Cell Biol. *167*, 1087–1098.
18. Merz, A.J., and Wickner, W.T. (2004). Resolution of organelle docking and fusion kinetics in a cell-free assay. Proc. Natl. Acad. Sci. USA *101*, 11548–11553.
19. Eitzen, G., Will, E., Gallwitz, D., Haas, A., and Wickner, W. (2000). Sequential action of two GTPases to promote vacuole docking and fusion. EMBO J. *19*, 6713–6720.
20. Seals, D.F., Eitzen, G., Margolis, N., Wickner, W.T., and Price, A. (2000). A Ypt/Rab effector complex containing the Sec1 homolog Vps33p is

required for homotypic vacuole fusion. Proc. Natl. Acad. Sci. USA *97*, 9402–9407.

21. Merz, A.J., and Wickner, W.T. (2004). Trans-SNARE interactions elicit Ca2+ efflux from the yeast vacuole lumen. J. Cell Biol. *164*, 195–206.

22. Thorngren, N., Collins, K.M., Fratti, R.A., Wickner, W., and Merz, A.J. (2004). A soluble SNARE drives rapid docking, bypassing ATP and Sec17/18p for vacuole fusion. EMBO J. *23*, 2765–2776.

23. Boeddinghaus, C., Merz, A.J., Laage, R., and Ungermann, C. (2002). A cycle of Vam7p release from and PtdIns 3-P-dependent rebinding to the yeast vacuole is required for homotypic vacuole fusion. J. Cell Biol. *157*, 79–89.

24. Starai, V.J., Jun, Y., and Wickner, W. (2007). Excess vacuolar SNAREs drive lysis and Rab bypass fusion. Proc. Natl. Acad. Sci. USA *104*, 13551–13558.

25. Luke, C.J., Pak, S.C., Askew, Y.S., Naviglia, T.L., Askew, D.J., Nobar, S.M., Vetica, A.C., Long, O.S., Watkins, S.C., Stolz, D.B., et al. (2007). An intracellular serpin regulates necrosis by inhibiting the induction and sequelae of lysosomal injury. Cell *130*, 1108–1119.

26. Haas, A. (1995). A quantitative assay to measure homotypic vacuole fusion. Methods Cell Sci. *17*, 283–294.